

RSC Advances



This is an *Accepted Manuscript*, which has been through the Royal Society of Chemistry peer review process and has been accepted for publication.

Accepted Manuscripts are published online shortly after acceptance, before technical editing, formatting and proof reading. Using this free service, authors can make their results available to the community, in citable form, before we publish the edited article. This *Accepted Manuscript* will be replaced by the edited, formatted and paginated article as soon as this is available.

You can find more information about *Accepted Manuscripts* in the [Information for Authors](#).

Please note that technical editing may introduce minor changes to the text and/or graphics, which may alter content. The journal's standard [Terms & Conditions](#) and the [Ethical guidelines](#) still apply. In no event shall the Royal Society of Chemistry be held responsible for any errors or omissions in this *Accepted Manuscript* or any consequences arising from the use of any information it contains.



Fabrication of Uniform Porous CNTs/Activated Carbon Composite Spheres by Oil-drop Method in Stratified Oils and Their Adsorption of VB₁₂

Received 00th January 2015,
Accepted 00th January 20xx

DOI: 10.1039/x0xx00000x

www.rsc.org/

Bingzhi Guo^{a,b,c,d}, Qianming Gong^{*a,b,c}, Junjie Wang^{a,b,c}, Yilun Huang^{a,b,c}, Daming Zhuang^{a,b,c} and Ji Liang^e

Presented is a flexible route to prepare uniform porous carbon nanotubes/activated carbon (CNTs/AC) composite spheres with high adsorption capacity. In this work, CNTs were firstly dispersed in ethanol aqueous solution of phenolic formaldehyde (PF) resin and then the transitional CNTs/PF composite spheres were synthesized by an oil-drop method. Meanwhile the CNT suspension drops were gradually cured in stratified oils with different densities. Subsequently, after being carbonized at 600 °C, steam activated at 800 °C and followed by alkali and deionized water wash, the resultant porous CNTs/AC composite spheres were acquired with CNTs of more than 65 wt%. Remarkably, the adsorption of VB₁₂ by the CNTs/AC composite spheres was as high as 60.36 mg/g, which was 4.32 and 3.96 times that of activated carbon beads and macroporous resin beads, respectively. Observations and microstructure analyses indicated that the good sphericity of the CNTs/AC spheres could be attributed to the suspended state of the CNTs/PF drops during curing which was supported by the stratified oils, and that the interconnected porous structure should be developed synergistically by ethanol and water evaporation during curing, carbonization of PF resin and activation of CNTs/AC spheres.

Introduction

Since their discovery in 1991, carbon nanotubes (CNTs) have been the subject of numerous research work given their unique properties¹. Nevertheless, some hindrance like limited length, poor dispersion, structure defects and poor interfacial bonding limited their application as structural materials²⁻³. Despite this, the crystal defects, which could act as active sites for functionalization, and the inherent aggregation or entanglement caused porous structure, together with the relatively high specific surface area, good chemical stability and excellent mechanical properties made CNTs a promising new adsorbent⁴⁻⁵. Actually, CNTs have been extensively studied as adsorbent for purification of drinking water sources and wastewater effluents⁶⁻⁹. All the results demonstrated the feasibility of CNTs to be used in environmental protection as a potential adsorbent⁵. Specifically, the multi-walled carbon nanotubes (MWNTs), not only had the unique hollow structure, but also could

form a large number of "aggregated pores"¹⁰, which made MWNTs exhibit much higher adsorption capacity for middle molecule toxins and rather higher adsorption rate compared with commercial activated carbon (AC) beads and macroporous resin (MR) beads used in hemoperfusion¹¹⁻¹³. These results demonstrated the possibility of CNTs to be developed as a new high efficient adsorbent in hemoperfusion¹⁴.

As a potential adsorbent, obviously, no matter in hemoperfusion or waste water treatment, CNTs could not be used in as-produced powdery state for possible secondary pollution and difficulty in recovery. Especially in hemoperfusion, the adsorbents should have suitable size, pore structure, high degree of sphericity and good blood compatibility. Compared with AC beads and MR beads presently used in hemoperfusion, CNTs based composite CNTs/AC microspheres were remarkable for their overwhelming adsorption capacity for VB₁₂ and low density lipoprotein (LDL)¹⁴⁻¹⁷. However, the adsorption capacity of CNTs/AC microspheres was discounted compared with the powdery CNTs for the ratio of CNTs in the composite microspheres was limited by the emulsion polymerization or the suspension polymerization method^{14,18-19}, in which the spherifying was determined by the surface tension of the binder resin. Once the ratio of CNTs exceeded about 45 wt%, good sphericity could not be obtained¹⁸. More unfavorable, suspension polymerization method would always result in a relatively wide

^a School of Materials Science and Engineering, Tsinghua University, Beijing 100084, P. R. China.

^b State Key Laboratory of New Ceramics and Fine Processing, Tsinghua University, Beijing 100084, P. R. China.

^c Key Laboratory for Advanced Materials Processing Technology, Ministry of Education, Beijing 100084, P. R. China.

^d Beijing Institute of Technology, Zhuhai, Zhuhai 519088, P. R. China.

^e Department of Mechanical Engineering, Tsinghua University, Beijing 100084, P. R. China.

Gaussian size distribution²⁰. Besides, some researchers took reverse microemulsion method to synthesize pure CNT spheres²¹. Because the spheres were self-assembled with the help of the limited electrostatic interaction among the functionalized CNTs, the size of the spheres were only about 2-20 μm and the shape was irregular mostly. In addition, some CNTs/Polymer composite microspheres of about 500 nm were synthesized by in-situ interfacial polymerization²². Although the tiny spheres exhibited distinguished electrochemical properties, no evidence indicated their potential utility as adsorbents. Similarly, some researchers successfully prepared hollow polyaniline/CNTs microspheres by incorporating template method and in-situ polymerization process, yet the resultant microspheres were only about 2-5 μm in diameter and the thickness of the shell was only about tens of nanometers²³. To sum up, as a competitive candidate for adsorption, CNTs based spheres could be further improved by increasing the ratio of CNTs in the composite spheres, enhancing the size and shape uniformity, and modifying the pore structure.

In this work, we proposed a flexible and convenient oil-drop method to prepare porous CNTs/AC composite spheres with high CNT ratio, hierarchical porous structure, uniform diameter and good sphericity. Actually, the oil-drop method not only conducted to modulate the ratio of CNTs in the composite spheres and homogenize the size of the spheres, but also the stratified oils with different densities helped to achieve good sphericity by maintaining the CNT suspension drops in suspended state during curing although the density of the drops would increase corresponding to the ethanol and water evaporation all the way in the hot oils. Otherwise, probably, the mixture drops would deform to be oblate spheroids if the drops plummeted directly to the bottom of the beaker before got hardening by curing. Further, vitamin B₁₂ was selected to evaluate the adsorption ability of the porous composite spheres with AC and MR beads used in hemoperfusion as the control samples.

Experimental

Materials

Acid-pretreated CNTs (Note: the CNTs used in this article were MWNTs with a purity of 98%) with the diameter of 8-15 nm, specific surface area of 150 m^2/g , the density is 1.20-2.10 g/m^3 and the surface oxygen content of about 6 % were provided by the Shanxi Guoneng New Material Co., Ltd (Beijing, china). Alcohol soluble phenol formaldehyde resin ($\rho=1.40\text{-}1.50 \text{ g}/\text{m}^3$) and curing agent paratoluensulfonyl chloride was obtained from Jining Baiyi Chemical Co., Ltd (Jining, china). Paraffin liquid (CP, $\rho=0.85 \text{ g}/\text{m}^3$) and Polydimethyl siloxane fluid (AR, $\rho=0.97 \text{ g}/\text{m}^3$) were purchased from the Tianjin Yongda Chemical Reagent Co., Ltd (Tianjin, china). Ethanol (AR, $\rho=0.79 \text{ g}/\text{m}^3$), Beijing Chemical Works (Beijing, china). Vitamin B₁₂ (biochemical reagent; Sinopharm Chemical Reagent Co., Ltd. Beijing, china) was used as the representative of middle molecular weight toxins according to the Chinese Industrial Standard of Hemoperfusion YY0464-2003. All other chemicals and

solvents were of analytical grade and used without further purification.

Preparation of CNTs/AC composite spheres

The typical synthesis process was illustrated in Scheme 1. Specifically, 1.0 g acid-pretreated CNTs and 3.0 g PF were dispersed in 40 ml ethanol solution (75 wt% of ethanol in deionized water). The suspension was sonicated for 2 h by ultrasonic crushing (KS-900F Kesheng Sonics Vibra Cell, 900 W, Ningbo Ultrasonic Equipment Co., Ltd, China) to improve the dispersion of CNTs in the solution. Then, before oil-drop process, 0.6 g curing agent (20 wt% of PF resin) and 15 ml ethanol were added into the CNTs/PF/ethanol/water mixture and CNTs/PF dispersion was obtained. Finally, the suspension was dropped into the two-phase system composed of paraffin liquid (PL) and polydimethyl siloxane fluid (PSF) at 70 $^\circ\text{C}$ by a syringe. After being cured in the stratified oils for 3 h, the spheres could keep shape. Then they were filtered and dried at 70 $^\circ\text{C}$ for another 2 h, the intermediate CNTs/PF composite spheres was obtained. Finally, the resultant porous CNTs/AC spheres were acquired by carbonizing the CNTs/PF spheres at 600 $^\circ\text{C}$ and activating the CNTs/carbon spheres at 800 $^\circ\text{C}$ with steam for 75 min in a tube furnace under an argon flow followed by a post-treatment of 1 M NaOH solution wash at 70 $^\circ\text{C}$ for 12 h and deionized water wash. After being dried at 80 $^\circ\text{C}$ for 2 h, the porous CNTs/AC composite spheres were ready for the next step. The CNT ratio of the resultant porous CNTs/AC composite spheres was about 50 wt%. With 1.8 g acid-pretreated CNTs and 3.0 g PF resin, the CNTs/AC spheres with about 65 wt% CNTs could be obtained.

Characterization

The morphology and microstructure of the spheres were observed with both MERLIN Compact field emission scanning electron microscope (SEM, Germany Carl Zeiss company) equipped with energy dispersive spectrum (EDS) analysis detectors and transmission electron microscopy (TEM, HT7700, HITACHI, Japan). The thermogravimetric analyses (TGA) were carried out on a Q5000IR thermoanalyzer (TA Instruments, USA) at a heating rate of 10 $^\circ\text{C}/\text{min}$ under nitrogen atmosphere. Nitrogen adsorption-desorption isotherms at 77 K from a Tristar 3020 II apparatus (USA Micromeritics) were used to calculate the specific surface area and pore size distribution with the Brunauer-Emmett-Teller (BET) method and Barrett-Joyner-Halen (BJH) method, respectively. Macropores were measured by Mercury porosimetry (AUTO PORE IV 9520) and the pressure range varied between 3.31×10^{-3} and $4.14 \times 10^2 \text{ MPa}$. The degree of sphericity and size distribution of the CNTs/AC composite spheres were analyzed by Image Analyser for 5051 which was developed by Tsinghua University.

Adsorption of VB₁₂

The adsorption tests were referred to the previous work of our group¹⁷⁻¹⁹. Specifically, 15 mg of the CNTs/AC spheres were added

into 50 ml of VB₁₂ solution (80 mg/L) and then they were shaken in a SHA-B shaker with a rotation speed of 150 rpm for 2 h at (37±1) °C. The solution was analyzed with a UV-Vis spectrophotometer (China) at a wavelength of (361±1) nm. The adsorption amount of VB₁₂ q (mg/g) was calculated by:

$$q = \left(\frac{C_0 - C_t}{W} \right) V$$

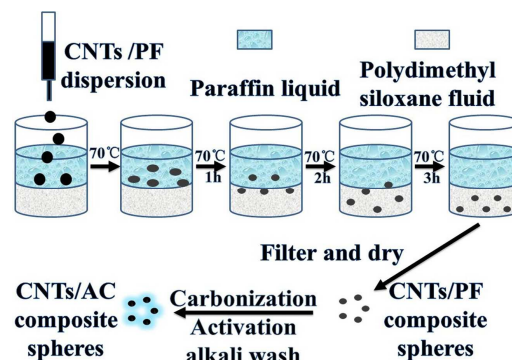
where C₀ and C_t were the VB₁₂ concentrations of the solution before adding the adsorbents and after 2 h of adsorption, respectively; V was the volume of the solution (50 ml); and W represented the weight of the sorbents.

Results and discussion

CNTs/AC spheres forming process and the pivotal role of the stratified oils

SEM images of CNTs/AC spheres before and after alkali wash were shown in Fig. 1. Its diameter was about 1.3 mm with good sphericity. Different from previous work, the spheres herein were prepared by a syringe injection instead of suspension polymerization or mechanical agitation. The sphericity of the original suspension drops could always be guaranteed by adjusting the viscosity of the suspension to make sure it could be dripped down. Since the spherification did not depend on the surface tension of the resin, the ratio of CNTs could be much higher than that reported before^{17,19}.

Before curing, the initial spherical suspension droplets were soft and easy to deform. On the one hand, if the density of the oil was much higher than that of the spherical droplets, they would float in the surface layer and deform to be ellipsoid by the interaction of their gravity and buoyancy. On the other hand, if the density of the oil was much lower than that of the droplets, they would plummet and crash into the bottom of the beaker to get deformed or fall apart. Therefore in this work, two layered-oil bath was designed. The density of upper PL matched that of initial suspension droplets thus it could keep the droplets in suspended state (Table 1). Since the initial spherical droplets were immersed in oil at 70 °C, most of the ethanol and water in them would evaporate and the density of the droplets would increase gradually. About 1 hour later, the droplets fell into PSF and in another 2 hours, the droplets would sink slowly to the bottom of the beaker. In this process, the droplets would shrink a little and the resin would get cured to some degree. It was reasonable to infer that the more the layers in the stratified oils, the more they matched the variation of the density of the droplets, thus the oils could keep the droplets in suspended state all the way. After being filtered and dried at 70 °C for another 2 hours, the intermediate CNTs/PF composite spheres were carbonized and activated (Fig.1a). It could be discerned that after carbonization and activation, the surface of the composite spheres was inlaid with some submicron sized beads (Fig.1b). Probably, this might be ascribed to the filling of PL or PSF into the space resulting from the evaporation of ethanol and water in the initial spheres. Based on TGA test results (Fig.2), it could be figured



Scheme 1 Schematic view of the synthetic procedure of the CNTs/AC composite spheres by the oil-drop method.

out that the weight loss of composite CNTs/PF spheres was about 22% higher than that of pure PF. Probably, this could be attributed to the adsorbed PL or PSF, which could be further verified by the EDS analysis of the submicron beads in the surface of CNTs/AC spheres (Inset of Fig.1b). The submicron beads were mainly silicon dioxide. As a whole, the weight losses after carbonization and activation were about 55 wt% and 30 wt%, respectively. Based on TGA tests, CNTs in the ultimate CNTs/AC spheres should be approximately 50 wt%.

After being washed by alkali solution, a lot of holes with the diameter of several micrometers emerged on the surface of CNTs/AC spheres (Fig.1c and d). Coincidentally, the adsorbed PL or PSF played the role of pore-forming agent in a certain extent. Predictably, these pores might be favorable for the diffusion of adsorbates.

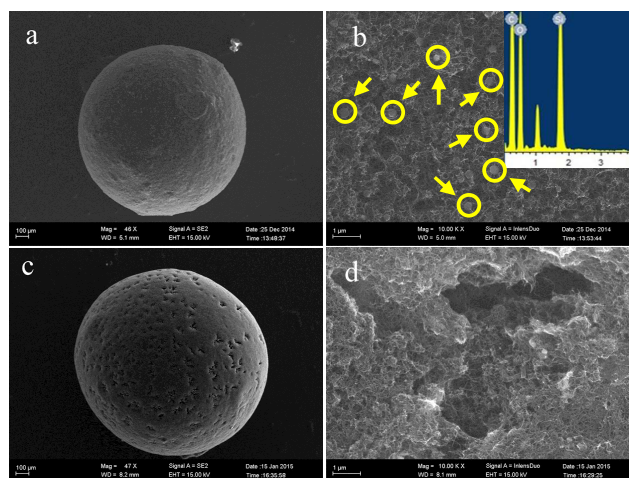


Fig.1 SEM images of CNTs/AC spheres before alkali wash (a) low and (b) high magnification, EDS spectrum of CNTs/AC spheres (b, inset), CNTs/AC spheres after alkali wash (c) low and (d) high magnification.

Table 1 The density of the different constituent in CNT suspension

| Constituents | H ₂ O | Ethanol | PF resin | CNTs | Suspension | PL | PSF |
|---------------------------|------------------|---------|-----------|-----------|------------|------|------|
| Density,g/cm ³ | 1.00 | 0.79 | 1.40~1.50 | 1.20~2.10 | 0.83~0.90 | 0.85 | 0.97 |

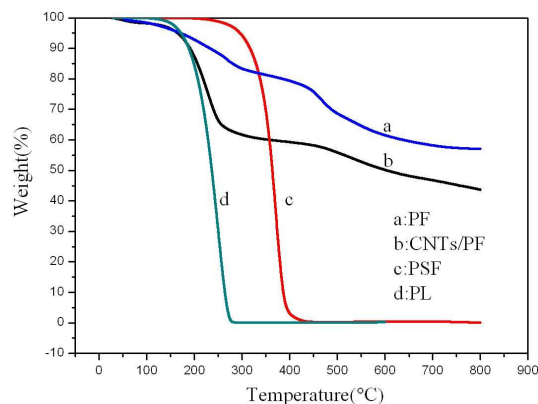


Fig. 2 TGA curves of PF, CNTs/PF, PSF and PL.

Size control and sphericity of the CNTs/AC spheres

The needle of the syringe could be of different size for controlling the size of the spheres. Three needles with different diameter were used to prepare CNTs/PF spheres. The diameters of the needles and the equivalent diameters microspheres were listed in Table 2. The macro-morphology and the size distribution of the spheres accomplished by Image Analyser for 5051 were demonstrated in Fig.3. It was clear that the size distribution was relatively concentrated and the diameters were in the range of 1.1 to 1.5 mm. While according to the equation of capillary diameter and droplet weight: $mg=2\pi r\gamma$, where m was the mass of the droplet, g was the acceleration of gravity, r was the external diameter of capillary and γ represented the surface tension, the ratio of the diameters of the droplets got by the three needles should be: 1.12:1.05:1, yet the actual data was 1.05:1.02:1. This could be ascribed to the shrink and deformation of the spheres during curing.

The shape of the sorbent is of great importance for hemoperfusion in clinic¹⁴. In this work, dimension ratio (DR), which was defined as the ratio of the minimum to the maximum of the diameter, and area ratio (AR), which was defined as the ratio of the projected area to the circumcircle area, were used to analyze the sphericity of the CNTs/AC spheres according to the Chinese national Standard GB/T 9441-1988. Spheroidization rate was calculated according to the same national standard which described the degree of sphericity statistically. For perfect spheres, the values of DR and AR should be 1.0 and Spheroidization rate should be 100%. The results in Table 3 indicated that the smaller the diameter of the needle, the higher the degree of sphericity for the spheres. This might be due to that the smaller the diameter of the needle, the smaller the mass of the droplet, the balance between the gravity and the surface tension could be easily

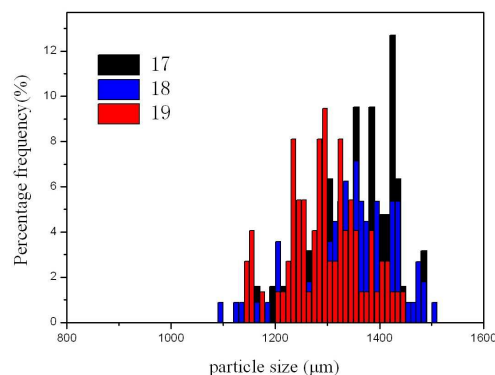
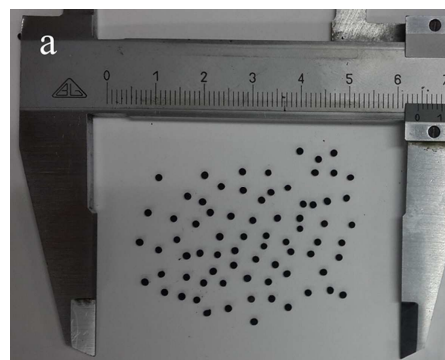


Figure.3 Optical image of CNTs/AC spheres by digital camera (a) and the size distribution (b).

Table 2 Needle parameters and microspheres equivalent diameters

| Needle type | Internal diameter (mm) | External diameter (mm) | Equivalent diameter of spheres (μm) |
|-------------|------------------------|------------------------|-------------------------------------|
| 17 | 1.12 | 1.48 | 1357 |
| 18 | 0.9 | 1.26 | 1326 |
| 19 | 0.7 | 1.06 | 1297 |

Table3 DR, AR and spheroidization rate of CNTs/AC spheres

| Needle type | DR | AR | Spheroidization rate(%) |
|-------------|------|------|-------------------------|
| 17 | 0.92 | 0.85 | 86 |
| 18 | 0.95 | 0.88 | 87 |
| 19 | 0.94 | 0.89 | 89 |

achieved in the oil bath. As for the larger droplets, they tended to deform into ellipsoids because of the predominant gravity compared with the surface tension, hence the density of the oil should be matched more to prevent the deformation of the initial uncured suspension drops.

Microstructure evolution and pore structure of CNTs/AC spheres

Before carbonization, CNTs in the CNTs/PF spheres was covered with PF resin and the spheres were almost voidless no matter in the surface or the inner zone (Fig.4a,b). The limited nano-sized pores in CNTs/PF spheres should come from the evaporation of ethanol and water during curing. While after being carbonized, not only the surface but the solid internal part turned into a porous structure (Fig.4c,d). Further activation would not alter the configuration of the pores by and large, nevertheless the CNTs got thinner (Fig5a,b) and definitely, the pore structure should be developed further (Fig.4e,f). Obviously, these irregular pores were mainly formed by the entanglement or stacking of the CNTs which

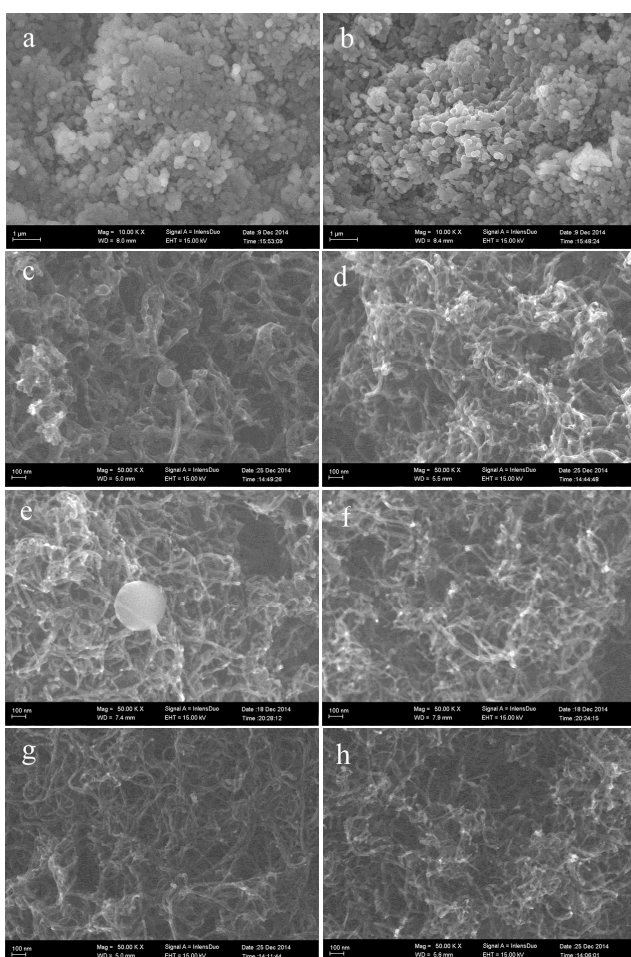


Fig.4 SEM images of appearant (a,c,e,g) and internal (b,d,f,h) morphology of CNTs/PF spheres (a and b), CNTs/PF spheres after Carbonization (c and d), CNTs/AC spheres before alkali wash (e and f) and after alkali wash (g and h).

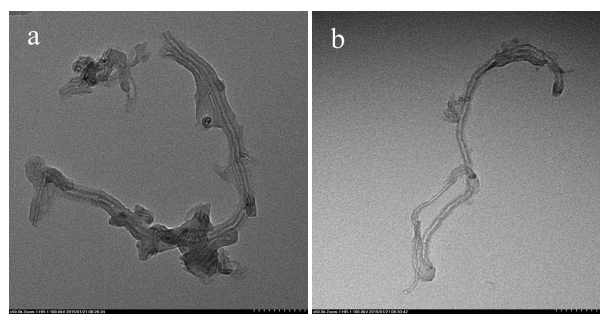


Fig.5 TEM images of CNTs coated with PF resin derived carbon before (a) and after activation (b).

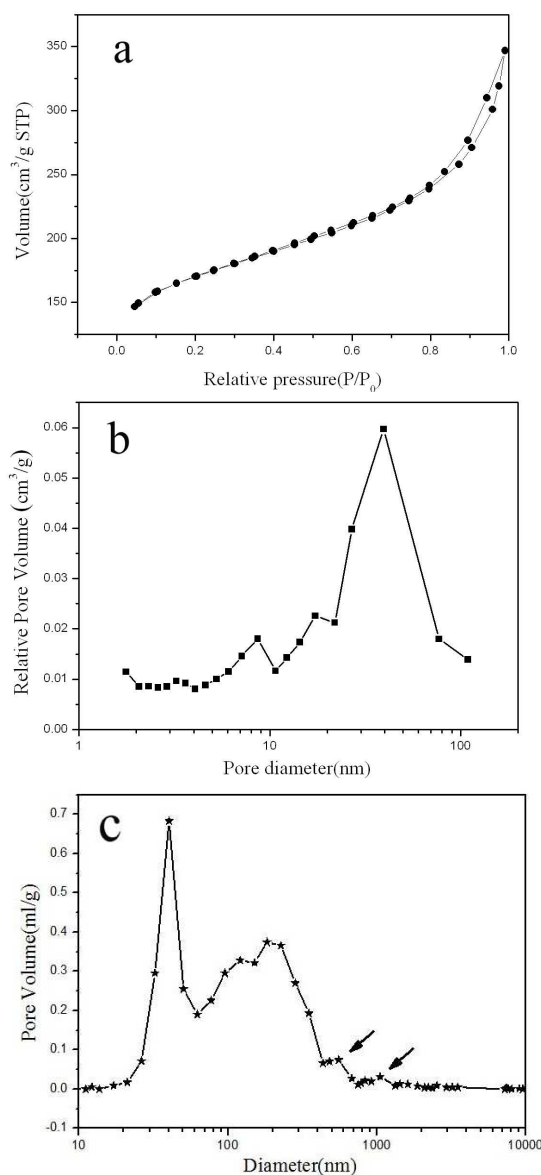


Fig.6 N₂ adsorption-desorption isotherm (a), pore diameter distribution of CNTs/AC spheres by BJH method (b) and pore distribution of the spheres by mercury porosimetry (c).

were "welded" by the PF derived carbon. In addition, the volatilization of alcohol and water during curing might be another approach to produce micropores. Since the curing process was accomplished in a suspended state, the CNTs were loosely connected with each other and this might be favorable for the formation of pore structure. Particularly, it was worth noting that the silica micro-beads inlaid in the surface of CNTs/AC spheres played the role of pore former coincidentally (Fig.4e), after being washed with alkali solution, uniform macropores with the diameter of several micrometers came out (Fig.4g and Fig.1d). This washing process did not change the inner pore structure of the spheres (Fig.4f,h). So far, a hierarchically porous structure including macropores, mostly in the surface, mesopores and micropores evolved from the volatilization of gaseous material during curing/carbonizing process and the entanglement among CNTs, came into being.

The nitrogen adsorption-desorption isotherms of the CNTs/AC spheres were shown in Fig.6a. It was evident that the isotherms were type IV curve, indicative of a multi-stage adsorption process. In the initial low relative pressure range ($p/p_0=0.15-0.45$), the isotherm went upward slowly, showing a surface monolayer adsorption process. In the medium relative pressure range ($p/p_0=0.45-0.85$), a small hysteresis suggested that the capillary occurred in small mesopores in a very narrow range ($3.0-4.0 \text{ nm}$)²⁴. By contrast, in the high relative pressure range ($p/p_0=0.85-0.99$), the adsorption of N_2 sharply increased, which indicated ultra-strong capillarity occurred in larger mesopores ($>20 \text{ nm}$) and macropores¹⁰. Exactly, the pore size distribution (Fig.6b) of a bimodal pattern was consistent with the analyses of adsorption/desorption isotherms above. The results showed that the average pore size of the resultant CNTs/AC composite spheres was approximately 8.1 nm. The total pore volume of the composite spheres was $0.354 \text{ cm}^3/\text{g}$. Besides, mercury (Hg) intrusion method was adopted to measure the macropores distribution of the CNTs/AC spheres. The result was shown in Fig.6c, which indicated that the median pore diameter was 40.7 nm (this was consistent with BJH results) and the macropores were mainly in the range of 100 nm to 400 nm. In addition, two small peaks at approximately 500 nm and 1 μm were in agreement with SEM observations (Fig.1c,d). The total pore volume obtained by this method was 4.7071 ml/g and the volume of macropores ($>50\text{nm}$) was 3.6256 ml/g . All these results demonstrated that the CNTs/AC spheres had a hierarchically porous structure. It was well known that before adsorption, the adsorbate should be accessible to the adsorption sites, thus the diffusion channels should be large enough¹⁷. VB_{12} was the representative of typical middle molecular weight toxins, its diameter was only about 2.09 nm, so the high adsorption capacity of VB_{12} by these porous CNTs/AC composite spheres should be expectable.

Adsorption of VB_{12}

Currently, AC beads and MR beads are the main adsorption materials applied in hemoperfusion. Fig.7 was the adsorption capacity for commercial AC beads, MR beads and CNTs/AC composites spheres with different ratios of CNTs. The adsorption of

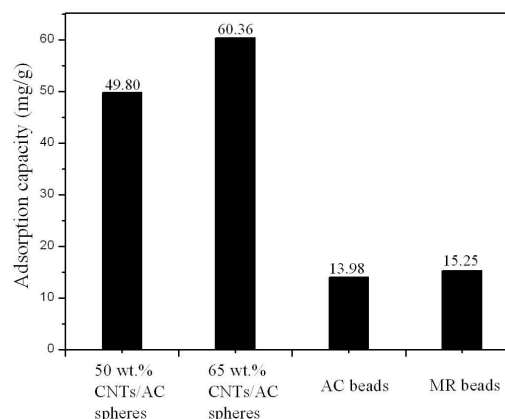


Fig.7 Adsorption of VB_{12} by CNTs/AC spheres, AC beads and MR beads.

VB_{12} in 2 h at 37°C for AC beads was 13.98 mg/g and that for MR beads was 15.25 mg/g . In contrast, the adsorption of VB_{12} by the CNTs/AC porous composite spheres with 50 wt% CNTs achieved 49.8 mg/g and further, the adsorption capacity for the 65 wt% CNTs sample was as high as 60.36 mg/g , which was 4.32 and 3.96 times as those of AC beads and MR beads, respectively (Fig.7). Albeit the specific areas of AC beads and MR beads were $810 \text{ cm}^2/\text{g}$ and $960 \text{ cm}^2/\text{g}$, which were rather higher than that of CNTs/AC spheres ($495 \text{ cm}^2/\text{g}$ for 50wt% CNTs sample), the pore structure was mainly microporous for AC beads and the pore distribution for MR beads was too single. The adsorption rate for the CNTs/AC beads was much higher than those for AC beads and MR beads. The difference about the adsorption rate of VB_{12} for these three adsorbents was very similar to our previous work⁵. Thus as a result, the highly developed mesopores and hierarchically porous structure in the CNTs/AC composite spheres would be more favorable for adsorption of the middle molecular weight VB_{12} .

Conclusions

In summary, a flexible method was developed to synthesize CNTs/AC porous composite spheres by an oil-drop method followed by gradual suspension curing in stratified oils. The CNTs/AC composite spheres had narrow diameter distribution and good sphericity for the persistent suspended state during curing. Besides, by this technology, the content of CNTs could be adjusted to more than 50 wt% in the composite spheres. In addition to the highly developed mesoporous structure brought about by the entanglement or stacking of CNTs, especially, the adsorbed oil during curing could act as macro-pore former and hence the hierarchically porous structure could be acquired. The adsorption capacity for the 65 wt% CNT sample was 60.36 mg/g , which was 4.32 and 3.96 times those of AC beads and MR beads and probably, these composite spheres could be another promising candidates for hemoperfusion.

Acknowledgements

We thanked Professor Xiang Chen in School of Materials Science and Engineering of Tsinghua University for his help in the diameter analyses of CNTs/AC composite spheres.

References

- 1 S. Nardecchia, D. Carriazo, M. L. Ferrer, M. C. Gutierrez and F. D. Monte, Three dimensional macroporous architectures and aerogels built of carbon nanotubes and/or graphene: synthesis and applications, *Chem. Soc. Rev.*, 2013, **42**, 794-830.
- 2 R.N. Ma, J.J. Hu, Z.W. Cai and H.X. Ju, Facile synthesis of boronic acid-functionalized magnetic carbon nanotubes for highly specific enrichment of glycopeptides, *Nanoscale*, 2014, **6**, 3150-3156.
- 3 C. Y. Tang, T. N. Zhou, J. H. Yang, Q. Zhang, F. Chen, Q. Fu and L. Yang, Wet-grinding assisted ultrasonic dispersion of pristine multi-walled carbon nanotubes (MWCNTs) in chitosan solution, *Colloids. Surf. B.*, 2011, **86**, 189-197.
- 4 A.H. Norzilah, A. Fakhru'l-Razi, T. S. Y. Choong and A. L. Chuah, Surface Modification Effects on CNTs Adsorption of Methylene Blue and Phenol, *J.Nanomater.*, 2011, 1-18.
- 5 J.J. Wang, Q. M. Gong, D. M. Zhuang and J. Liang, Chemical vapor infiltration tailored hierarchical porous CNTs/C composite spheres fabricated by freeze casting and their adsorption properties, *RSC Adv.*, 2015, **5**(22), 16870-16877.
- 6 S. Z. Li, Y. B. Gong, Y. C. Yang, C. He, L. L. Hu, L. F. Zhu, L. P. Sun and D. Shu, Recyclable CNTs/Fe₃O₄ magnetic nanocomposites as adsorbents to remove bisphenol A from water and their regeneration, *Chem. Eng. J.*, 2015, **260**, 231-239.
- 7 G. P. Rao, C. Y. Lu and F. S. Su, Sorption of divalent metal ions from aqueous solution by carbon nanotubes: A review, *Sep Purif. Technol.*, 2007, **58**, 224-231.
- 8 J. N. Zhang, Z. H. Huang, R. T. Lv, Q. H. Yang and F. Y. Kang, Effect of Growing CNTs onto Bamboo Charcoals on Adsorption of Copper Ions in Aqueous Solution, *Langmuir*, 2009, **25**, 269-274.
- 9 J. Ma, Z. L. Zhu, B. Chen, M. X. Yang, H. M. Zhou, C. Li, F. Yu and J. H. Chen, One-pot, large-scale synthesis of magnetic activated carbon nanotubes and their applications for arsenic removal, *J. Mater. Chem. A.*, 2013, **1**, 4662-4666.
- 10 Q. H. Yang, P. X. Hou, S. Bai, M. Z. Wang and H. M. Cheng, Adsorption and capillarity of nitrogen in aggregated multi-walled carbon nanotubes, *Chem. Phys. Lett.*, 2001, **345**, 18-24.
- 11 J. J. Miao, F. M. Zhang, M. Takiuddin, S. Mousa and R. J. Linhardt, Adsorption of Doxorubicin on Poly(methyl methacrylate)-Chitosan-Heparin-Coated Activated Carbon Beads, *Langmuir*, 2012, **28**, 4396-4403.
- 12 C. Ye, Q. M. Gong, F. P. Lu and J. Liang, Adsorption of uraemic toxins on carbon nanotubes, *Sep. Purif. Technol.*, 2007, **58**, 2-6.
- 13 C. A. Howell, S. R. Sandeman, G. J. Phillips, S. V. Mikhailovsky, S. R. Tennison, A. P. Rawlinson and O. P. Kozynchenko, Nanoporous activated carbon beads and monolithic columns as effective hemoadsorbents for inflammatory cytokines, *Int. J. Artif. Organs.*, 2013, **36**(9), 624-632.
- 14 Y. M. Lu, Q. M. Gong, F. P. Lu, J. Liang, L. J. Ji, Q. D. Nie and X. M. Zhang, Preparation of sulfonated porous carbon nanotubes/activated carbon composite beads and their adsorption of low density lipoprotein, *J. Mater. Sci.: Mater. Med.*, 2011, **22**, 1855-1862.
- 15 D. J. Malik, G. L. Warwick, I. Mathieson, N. A. Hoenich and M. Streat, Structured carbon haemoadsorbents for the removal of middle molecular weight toxins, *Carbon*, 2005, **43**, 2317-2329.
- 16 D. J. Malik, G. L. Warwick, M. Venturi, M. Streat, K. Hellgardt, N. Hoenich and J. A. Dale, Preparation of novel mesoporous carbons for the adsorption of an inflammatory cytokine (IL-1b), *Biomaterials*, 2004, **25**, 2933-2940.
- 17 C. Ye, Q. M. Gong, F. P. Lu and J. Liang, Preparation of carbon nanotubes/phenolic-resin-derived activated carbon spheres for the removal of middle molecular weight toxins, *Sep. Purif. Technol.*, 2008, **61**, 9-14.
- 18 Y. M. Lu, Q. M. Gong and J. Liang, Preparation of Carbon Nanotubes/Activated Carbon Composite Microspheres and Their Application to Adsorption of VB₁₂, *Acta Phys.-Chim. Sin.*, 2009, **25**(8), 1697-1702.
- 19 Y. M. Lu, Q. M. Gong, F. P. Lu and J. Liang, Synthesis of porous carbon nanotubes/activated carbon composite spheres and their application for vitamin B12 adsorption, *Sci. Eng. Compos. Mater.*, 2014, **21**(2), 165-171.
- 20 P. J. Dowling and B. Vincent, Suspension polymerisation to form polymer beads, *Colloid. Surf. A.*, 2000, **161**, 259-269.
- 21 Y. Q. Liu, X. H. Chen, K. Zhang, B. Yi, W. Wang and L. P. Zhou, Synthesis of carbon nanotube microspheres by reverse microemulsion, *J. Inorg. Mater.*, 2009, **24**(5) 993-997.
- 22 P. Liu, X. Wang and H. L. Li, Preparation of carboxylated carbon nanotubes/polypyrrole composite hollow microspheres via chemical oxidative interfacial polymerization and their electrochemical performance, *Synthetic. Met.*, 2013, **181**, 72-78.
- 23 C. Yang, P. Liu, P. C. Du and X. Wang, Stabilization of carbon nanotubes-based hollow cages for energy storage: From collapsed morphology to free-standing structure, *Electrochim. Acta.*, 2013, **105**, 53-61.
- 24 P. Ariyadejwanich, W. Tanthapanichakoon, K. Nakagawa, S.R. Mukai and H. Tamon, Preparation and characterization of mesoporous activated carbon from waste tires, *Carbon*, 2003, **41**, 157-164.